

Learning Phase Transitions from Regression Uncertainty

Wei-chen Guo and Liang He*

*Guangdong Provincial Key Laboratory of Quantum Engineering and Quantum Materials,
School of Physics and Telecommunication Engineering,
South China Normal University, Guangzhou 510006, China and
Guangdong-Hong Kong Joint Laboratory of Quantum Matter,
South China Normal University, Guangzhou 510006, China*

For performing regression tasks involved in various physics problems, enhancing the precision, or equivalently reducing the uncertainty of the regression results is undoubtedly one of the central goals. Here, somewhat surprisingly, we find that the unfavorable regression uncertainty in performing regression tasks of inverse statistical problems actually contains “hidden” information concerning phase transitions of the system under consideration. By utilizing this “hidden” information, we develop a new unsupervised machine learning approach dubbed “learning from regression uncertainty” for automated detection of phases of matter, with the core working horse being a neural network performing regression tasks instead of classification tasks as in various related machine learning approaches developed so far. This is achieved by revealing an intrinsic connection between regression uncertainty and response properties of the system under consideration, thus making the results of this machine learning approach directly interpretable. We demonstrate the approach by identifying the critical point of the ferromagnetic Ising model and revealing the existence of the intermediate phase in the six-state and seven-state clock models. Our approach paves the way towards intriguing possibilities for unveiling new physics via machine learning in an interpretable manner.

Introduction.—In recent years, the artificial neural network (NN) based machine learning techniques have stimulated the rapid development of automated data-driven approaches to investigate a wide range of physics problems [1–3]. As one of the central classes of problems in condensed matter physics, classifying phases of matter and identifying phases transitions is a major focus of applying machine learning. In particular, a considerable number of approaches utilizing the power of NNs in performing classification tasks have been developed and succeeded in providing data-driven evidence on the existence of various phase transitions [4, 5], such as the phase transitions associated with nonequilibrium self-propelled particles [6, 7], topological defects [8–11], many-body localization [12, 13], strongly correlated fermions [14, 15], etc. And besides the widely-involved classification tasks, there is yet another fundamental class of tasks that can be dealt with efficiently by modern machine learning techniques, namely, regression tasks [16]. In fact, applying the machine learning techniques designed for regression tasks to physics problems is giving rise to a burgeoning field towards automated theory building, where, for instance, the symbolic regression [17–19] has been successfully applied to extract the equations of motion [20], symmetries [21], and conservation laws [22] from various types of data of physical systems.

But despite the exciting development in this context, a quite natural application scenario of machine learning techniques has received little attention so far, namely, classifying phases of matter and identifying phases transitions by utilizing the power of NNs in performing regression tasks. Currently, to classify phases and identify

phase transitions with machine learning, the existing approaches usually train the NN to perform a certain classification task [4, 5]. In spite of their successes, they generally face the lack of interpretability as the classes of patterns recognized by them are essentially abstract, hence assume no straightforward relation to the conventional notions of physics [1–3, 23–29]. In contrast, for the NNs designed for regression tasks, the precisely interpretable meaning of their outputs can usually be traced back to the regression tasks themselves straightforwardly. Taking the NNs designed for solving the inverse statistical problem (ISP) [30] for example, they are trained to perform the prototypical regression tasks of reconstructing certain system parameters from given samples of observed system configurations, with their outputs naturally holding the same meaning as the system parameters they try to reconstruct. In these regards, the power of NNs in performing regression tasks might shed new light on automated detection of phases of matter. This thus raises the fundamental and intriguing question of whether and how phase transitions can be unsupervisedly revealed by NN-based regression.

Here, we address this question for prototypical regression tasks in ISP performed by NNs. In previous investigations [30–40], enhancing the precision, or equivalently reducing the uncertainty of the regression results has been regarded as one of the central goals. However, somewhat surprisingly, we find this unfavorable regression uncertainty actually contains “hidden” information that can be utilized to reveal possible phase transitions of the system under consideration. As shown in the case of the ferromagnetic Ising model, the position of the minimum of regression uncertainty directly corresponds to the critical point of the ferromagnetic phase transition of the system [cf. Fig. 1(b)]. By utilizing this “hidden” information, we

* liang.he@sncu.edu.cn

develop a new unsupervised machine learning approach dubbed “learning from regression uncertainty” (LFRU) for automated detection of phases of matter, with the core working horse being an NN performing regression tasks instead of classification tasks as in various related machine learning approaches developed so far [4–15, 41–45]. This is achieved by revealing an intrinsic connection between regression uncertainty and response properties of the system under consideration [cf. Fig. 1(c)], thus making the results of this machine learning approach directly interpretable. By utilizing the unsupervised characteristic and the interpretability of LFRU, we provide a new type of data-driven evidence on the existence of the intermediate phase in the six-state and seven-state clock models, and data-driven evidence that the transitions in these systems are not of the Landau type (cf. Fig. 2). Moreover, since the implementation of this approach is robust against different choices of the NN architecture, we believe that state-of-art developments in the field of artificial intelligence and data science can be readily exploited to automatically detect phases of matter in an interpretable manner via LFRU.

Identify phase transitions from “hidden” information in regression uncertainty.—To see concretely how the uncertainty of the regression results (regression uncertainty) in ISP can be utilized to reveal possible phase transitions, let us start with ISP in the prototypical ferromagnetic Ising model $H = -J \sum_{\langle i,j \rangle} s_i s_j$, where spins $s_i = \pm 1$ are located on a square lattice with linear size L and periodic boundary condition imposed. And we set the coupling strength $J = 1$ as the energy unit in the following.

As the inverse of generating spin configurations that satisfy the probability distribution $\exp(-H/T)/Z$ ($Z \equiv \sum_{\{s_i\}} \exp(-H/T)$ and the Boltzmann constant k_B is set to be 1) at a given temperature T , the ISP in this case asks the question of what the possible temperature is for a given spin configuration [cf. Fig. 1(a)], hence naturally corresponds to a prototypical regression task. We perform this regression task by training the NN as an $L \times L \rightarrow 1$ map from the set of spin configurations to the set of reconstructed temperatures denoted by T_R . During the training process of the NN, a large number of its parameters are optimized by minimizing the mean square error loss function [16]

$$\mathbb{L} \equiv \langle (T - T_R)^2 \rangle, \quad (1)$$

where $\langle \cdot \rangle$ denotes the average over all the samples in the training dataset (see Supplemental Material [46] for technical details concerning the training). Noticing that due to the intrinsic statistical characteristic of ISP, for any set of spin configurations, i.e., samples, generated at a given temperature T according to the probability distribution $\exp(-H/T)/Z$, some of its spin configurations can also appear in other sets of spin configurations generated at temperatures that are different from T , and thus the reconstructed temperatures T_R for each spin configuration in the same set generally does not assume the same value, which gives rise to intrinsic uncertainty of the regression

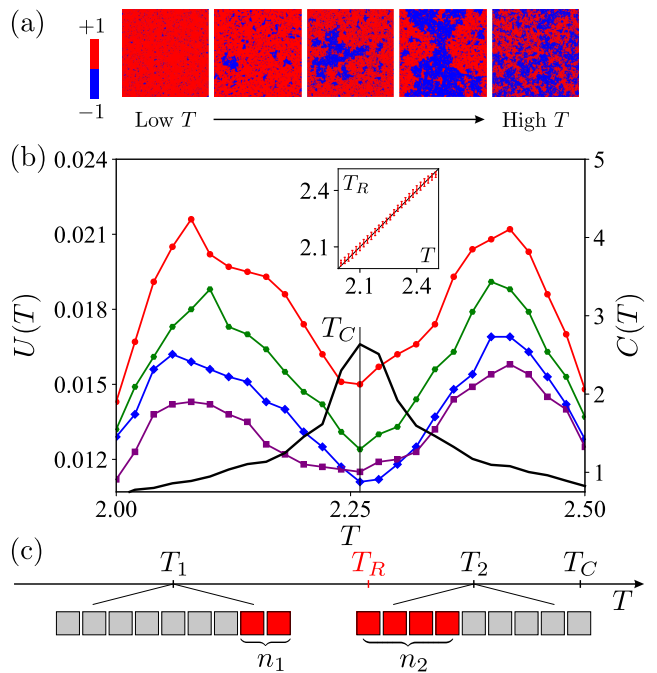


Figure 1. Learning the Ising transition from regression uncertainty. (a) Typical real-space configurations (samples processed directly by the NN) of the ferromagnetic Ising model. (b) Temperature dependence of regression uncertainty $U(T)$ for the ferromagnetic Ising model with the linear system size $L = 120$ (red), $L = 140$ (green), $L = 160$ (blue), and $L = 180$ (purple). The curve of regression uncertainty $U(T)$ assumes a non-trivial M-shape and the valley appears at $T = 2.26 \pm 0.01$ which matches the critical temperature $T_C \approx 2.269$, suggesting that it contains non-trivial information, i.e., the position of the valley, which can be utilized to reveal possible phase transitions. The black curve corresponds to the temperature dependence of the system’s heat capacity $C(T)$ with $L = 180$. Inset: Regression results of a well-trained NN for the corresponding ISP with $L = 120$. The reconstructed temperature T_R (red) is very close to the target T (black diagonal line), but there always exists an intrinsic regression uncertainty $U(T)$ as shown by the error bars. (c) Schematic illustration of the origin of the “hidden” information in regression uncertainty. During training, two sets of an equal number of samples (squares) generated at two different temperatures T_1 and T_2 ($T_1 < T_2 < T_C$) are provided to the NN. n_1 samples (red squares) that correspond to relatively high energy in the set of T_1 can be essentially indistinguishable from n_2 samples (red squares) that correspond to relatively low energy in the set of T_2 . One expects $n_2 > n_1$ since the response property of the system with respect to the temperature, i.e., the heat capacity that characterizes the strength of thermal fluctuations satisfies $C(T_2) > C(T_1)$. To achieve an overall good performance in reconstructing the temperature, the reconstructed temperature T_R for these samples (red squares) is closer to T_2 rather than T_1 , giving rise to $U(T_2) < U(T_1)$. In particular, the temperature at which the heat capacity $C(T)$ reaches its maximum should match exactly the temperature at which the regression uncertainty $U(T)$ reaches its minimum as shown in (b). This reveals the intrinsic connection between regression uncertainty and response properties that gives rise to “hidden” information in the regression uncertainty. See text for more details.

results. Straightforwardly, one can use the standard deviation $U(T)$ of well-trained NN's outputs to characterize this regression uncertainty at a given temperature T ,

$$U(T) \equiv \sqrt{\langle (T_R - \langle T_R \rangle_T)^2 \rangle_T}, \quad (2)$$

where $\langle \cdot \rangle_T$ denotes the average over all the samples generated at T in the test dataset. For instance, as we can see from the error bars in the inset of Fig. 1(b), although the regression uncertainty $U(T)$ can be generally very small for the well-trained NN that assumes good performance in reconstructing the temperature, it always exists.

Naturally, the regression uncertainty is unfavorable for reconstructing the precise temperature T from given spin configurations. However, somewhat surprisingly, we find that it actually contains “hidden” information that can be utilized to identify the critical point T_C of the ferromagnetic phase transition of the system. As we can see from Fig. 1(b), the temperature dependence of regression uncertainty $U(T)$ assumes a non-trivial M-shape in this case. With a detailed check at its valley position, one in fact can find the valley appears at $T = 2.26 \pm 0.01$ which matches the critical temperature $T_C \approx 2.269$ [47] of the two-dimensional ferromagnetic Ising model very well. This strongly suggests that the temperature dependence of regression uncertainty $U(T)$ contains non-trivial information, i.e., the position of the valley, which can be utilized to reveal possible phase transitions.

To further see the origin of this non-trivial information in regression uncertainty, let us consider the training process of the NN fed with two sets of an equal number of samples that are generated at two different temperatures T_1 and T_2 , respectively. Without losing generality, one can assume $T_1 < T_2 < T_C$ [cf. Fig. 1(c)]. Since the samples in these two sets are generated probabilistically, one expects that certain amount of samples, say n_1 samples, that correspond to relatively high energy in the set of T_1 are essentially indistinguishable from certain amount of samples, say n_2 samples, that correspond to relatively low energy in the set of T_2 [cf. the red squares in Fig. 1(c)]. To achieve an overall good performance in reconstructing the temperature, one expects that in the training process, the NN minimizes the loss function \mathbb{L} by associating the reconstructed temperature $T_R = (n_1 T_1 + n_2 T_2) / (n_1 + n_2)$ to these essentially indistinguishable samples. Further noticing that thermal fluctuations at T_2 are stronger than T_1 due to $T_1 < T_2 < T_C$, one thus expects $n_2 > n_1$, since the samples with their energy deviating from the average energy of the set are more easily accessed by stronger thermal fluctuations. As a result, the reconstructed temperature T_R for these essentially indistinguishable samples is closer to T_2 rather than T_1 , giving rise to a smaller regression uncertainty at T_2 compared to the one at T_1 , i.e., $U(T_2) < U(T_1)$. Moreover, the strength of thermal fluctuations at different temperature T can be characterized by the response property of the system with respect to the temperature, i.e., by the heat capacity $C(T) = (\langle H^2 \rangle - \langle H \rangle^2) / NT^2$. This indicates that a larger heat capacity corresponds to

a smaller regression uncertainty, and in particular, the temperature at which the heat capacity $C(T)$ reaches its maximum should match exactly the temperature at which the regression uncertainty $U(T)$ reaches its minimum. As we can see from the heat capacity curve in Fig. 1(b), the temperature of the peak of $C(T)$ indeed assumes the same value as the one of the valley of $U(T)$.

This thus reveals an intrinsic connection between regression uncertainty and response properties of the system, which can be utilized to establish a new type of unsupervised machine learning approach for revealing possible phase transitions that we refer to as “learning from regression uncertainty” (LFRU). In this approach, one does not need to resort to any prior built-in physical knowledge concerning phase transitions of the system under consideration. As already shown concretely in the case of the ferromagnetic Ising model, one directly trains the NN to perform regression tasks of the corresponding ISP and then calculates the regression uncertainty of the well-trained NN afterward [cf. Eq. (2) for instance]. By the non-trivial minima of regression uncertainty, the key information concerning possible phase transitions is unsupervisedly revealed. For continuous phase transitions, the corresponding response functions diverge (reach their maxima for systems of finite sizes) at critical points, so the positions of the minima of regression uncertainty directly correspond to the critical points of phase transitions [cf. Fig. 1(b) for instance]. Moreover, noticing that LFRU does not assume the number of existing phases in the system under consideration, one could directly use it to investigate complex physical systems with possible intermediate phases [48–53]. As we shall see in the concrete example presented in the following, LFRU can indeed reveal the key information concerning intermediate phases.

Reveal intermediate phases from regression uncertainty and its limitation.—Let us now discuss how phase transitions in systems with possible intermediate phases can be investigated by LFRU. To this end, we consider the q -state clock model $H_q = -J \sum_{\langle i,j \rangle} \cos(\theta_i - \theta_j)$, where $\theta_i = 2\pi n_i / q$ denotes the q -valued spin located at the lattice site i with $n_i = 0, 1, \dots, q-1$. It reduces to the Ising model when $q = 2$ and the XY model when $q \rightarrow \infty$. Here, we focus on the $q = 6, 7$ cases, which exhibit an intermediate vortex-antivortex condensed Berezinskii-Kosterlitz-Thouless (BKT) phase between paramagnetic and ferromagnetic phases [54–56].

To investigate the temperature-driven phase transitions in the six-state and seven-state clock models, we first train the NN to perform the ISP regression for reconstructing the temperature T in these two models and calculate their respective regression uncertainty. As we can see from the temperature dependence of regression uncertainty $U(T)$ shown in Fig. 2, both the $U(T)$ curves assume two successive M-shapes. Such a structure with two non-trivial minima, instead of one, is in sharp contrast to the one for the Ising model presented in Fig. 1(b), indicating that the six-state and seven-state clock models assume three different phases, i.e., an intermediate

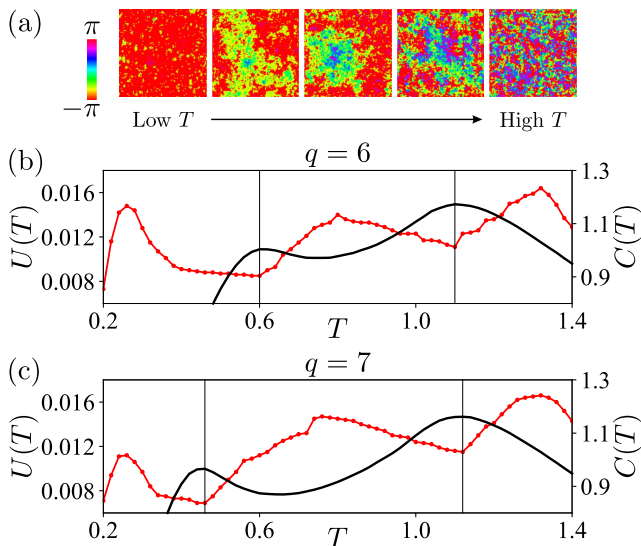


Figure 2. Revealing the intermediate phase in the q -state clock models from regression uncertainty. (a) Typical real-space configurations (samples processed directly by the NN) of the six-state clock model. (b) Temperature dependence of regression uncertainty $U(T)$ for the six-state clock model with the linear system size $L = 100$. The curve of regression uncertainty $U(T)$ (red curve) assumes two successive M-shapes, indicating that the six-state clock model assumes three different phases, i.e., an intermediate phase that is absent in its two-state Ising counterpart. The positions of the two minima of the regression uncertainty $U(T)$ correspond to the two maxima of the response function associated with the temperature, i.e., the heat capacity $C(T)$ (black curve), hence not the BKT transition points in this system [61–63]. (c) Analogous data to (b), but for the seven-state clock model. See text for more details.

phase that is absent in their two-state Ising counterpart. This thus provides a new type of data-driven evidence on the existence of the intermediate phase in these two models, corroborating the results in previous investigations employing conventional approaches such as the ones utilizing the helicity modulus [57, 58], the Fisher zeros [59, 60], the entanglement entropy of the fixed-point matrix-product-state [61], etc.

At this stage one may incline to associate the two minima of regression uncertainty $U(T)$ shown in Fig. 2(b) or Fig. 2(c) to the two transition points of the six-state or seven-state clock model. But thanks to the interpretability of LFRU, we know that the two minima of regression uncertainty $U(T)$ should correspond to the two maxima of the response function associated with the temperature, i.e., the heat capacity $C(T)$, which is indeed the case as shown by the vertical lines in Fig. 2(b) and Fig. 2(c). Noticing that the phase transitions associated with the intermediate phase in these two models are of the BKT type, i.e., driven by topological defects [61–63], the po-

sitions of the two maxima of heat capacity $C(T)$ in fact do not exactly match the critical temperatures [61], indicating that the positions of the two minima of regression uncertainty $U(T)$ in Fig. 2(b) and Fig. 2(c) should not be interpreted as the BKT transition points. This on the one hand clarifies that quantitatively identifying critical points via LFRU is restricted to continuous phase transitions, and on the other hand provides data-driven evidence that the transitions in these systems are not of the Landau type, corroborating recent investigations [61–63].

Finally, we remark that the implementation of LFRU is robust against different choices of the NN architecture. All the machine learning results presented in Fig. 1 and Fig. 2 are obtained by employing a widely-used standard NN called “ResNet” [64]. In Supplemental Material [46], we present the same analysis employing another type of widely-used standard NN called “GoogLeNet” [65], and their corresponding results agree very well with each other. This suggests that state-of-art developments in the field of artificial intelligence and data science can be readily exploited to automatically detect phases of matter in an interpretable manner via LFRU.

Conclusions.—Despite being unfavorable for enhancing the precision of the regression results in ISP, the regression uncertainty assumes an intrinsic connection to response properties of the system under consideration, making it accommodate crucial information of the system’s possible phase transitions. This enables the development of a fundamentally new type of generic unsupervised machine learning approach LFRU for automated detection of phases of matter, which is based on regression instead of classification and produces directly interpretable results, as manifested concretely in the cases of Ising model and six-state and seven-state clock models. Noticing that the working mechanism of LFRU is quite general, its application is not restricted to temperature-driven transitions investigated here. Moreover, possible phase transitions in nonequilibrium complex many-body systems such as systems consisting of self-propelled particles [3, 66–69] can also be investigated via this approach. We believe that our findings will stimulate further efforts in both developing and applying interpretable machine learning approaches to unveil new physics in both equilibrium and nonequilibrium complex many-body systems.

ACKNOWLEDGMENTS

This work was supported by NSFC (Grants No. 11874017), GDSTC (Grants No. 2018A030313853), Major Basic Research Project of Guangdong Province (Grant No. 2017KZDXM024), Science and Technology Program of Guangzhou (Grant No. 2019050001), and START grant of South China Normal University.

-
- [1] G. Carleo, I. Cirac, K. Cranmer, L. Daudet, M. Schuld, N. Tishby, L. Vogt-Maranto, and L. Zdeborová, *Rev. Mod. Phys.* **91**, 045002 (2019).
- [2] J. Carrasquilla, *Adv. Phys. X* **5**, 1797528 (2020).
- [3] F. Cichos, K. Gustavsson, B. Mehlig, and G. Volpe, *Nat. Mach. Intell.* **2**, 94 (2020).
- [4] J. Carrasquilla and R. G. Melko, *Nat. Phys.* **13**, 431 (2017).
- [5] E. P. L. van Nieuwenburg, Y.-H. Liu, and S. D. Huber, *Nat. Phys.* **13**, 435 (2017).
- [6] J. Venderley, V. Khemani, and E.-A. Kim, *Phys. Rev. Lett.* **120**, 257204 (2018).
- [7] W.-C. Guo, B.-Q. Ai, and L. He, *Phys. Rev. E* **104**, 044611 (2021).
- [8] M. J. S. Beach, A. Golubeva, and R. G. Melko, *Phys. Rev. B* **97**, 045207 (2018).
- [9] P. Suchsland and S. Wessel, *Phys. Rev. B* **97**, 174435 (2018).
- [10] S. S. Lee and B. J. Kim, *Phys. Rev. E* **99**, 043308 (2019).
- [11] M. N. Chernodub, H. Erbin, V. A. Goy, and A. V. Molochkov, *Phys. Rev. D* **102**, 054501 (2020).
- [12] F. Schindler, N. Regnault, and T. Neupert, *Phys. Rev. B* **95**, 245134 (2017).
- [13] Y.-T. Hsu, X. Li, D.-L. Deng, and S. Das Sarma, *Phys. Rev. Lett.* **121**, 245701 (2018).
- [14] K. Ch'ng, J. Carrasquilla, R. G. Melko, and E. Khatami, *Phys. Rev. X* **7**, 031038 (2017).
- [15] P. Broecker, J. Carrasquilla, R. G. Melko, and S. Trebst, *Sci. Rep.* **7**, 1 (2017).
- [16] I. Goodfellow, Y. Bengio, and A. Courville, *Deep Learning* (MIT Press, Cambridge, 2016).
- [17] S.-M. Udrescu and M. Tegmark, *Sci. Adv.* **6**, eaay2631 (2020).
- [18] T. Wu and M. Tegmark, *Phys. Rev. E* **100**, 033311 (2019).
- [19] Z. Liu, B. Wang, Q. Meng, W. Chen, M. Tegmark, and T.-Y. Liu, *Phys. Rev. E* **104**, 055302 (2021).
- [20] S.-M. Udrescu and M. Tegmark, *Phys. Rev. E* **103**, 043307 (2021).
- [21] Z. Liu and M. Tegmark, arXiv:2109.09721.
- [22] Z. Liu and M. Tegmark, *Phys. Rev. Lett.* **126**, 180604 (2021).
- [23] D. E. Gökmen, Z. Ringel, S. D. Huber, and M. Koch-Janusz, *Phys. Rev. Lett.* **127**, 240603 (2021).
- [24] D. E. Gökmen, Z. Ringel, S. D. Huber, and M. Koch-Janusz, *Phys. Rev. E* **104**, 064106 (2021).
- [25] W. Zhang, L. Wang, and Z. Wang, *Phys. Rev. B* **99**, 054208 (2019).
- [26] S.-H. Li and L. Wang, *Phys. Rev. Lett.* **121**, 260601 (2018).
- [27] H.-Y. Hu, S.-H. Li, L. Wang, and Y.-Z. You, *Phys. Rev. Research* **2**, 023369 (2020).
- [28] C. Miles, A. Bohrdt, R. Wu, C. Chiu, M. Xu, G. Ji, M. Greiner, K. Q. Weinberger, E. Demler, and E.-A. Kim, *Nat. Commun.* **12**, 3905 (2021).
- [29] C. Miles, R. Samajdar, S. Ebadi, T. T. Wang, H. Pichler, S. Sachdev, M. D. Lukin, M. Greiner, K. Q. Weinberger, and E.-A. Kim, arXiv:2112.10789.
- [30] H. C. Nguyen, R. Zecchina, and J. Berg, *Adv. Phys.* **66**, 197 (2017).
- [31] E. Aurell and M. Ekeberg, *Phys. Rev. Lett.* **108**, 090201 (2012).
- [32] H. C. Nguyen and J. Berg, *Phys. Rev. Lett.* **109**, 050602 (2012).
- [33] A. Decelle and F. Ricci-Tersenghi, *Phys. Rev. E* **94**, 012112 (2016).
- [34] C. Donner and M. Opper, *Phys. Rev. E* **96**, 062104 (2017).
- [35] P. Contucci, R. Luzzi, and C. Vernia, *J. Phys. A: Math. Theor.* **50**, 205002 (2017).
- [36] J. Jo, D.-T. Hoang, and V. Periwal, *Phys. Rev. E* **101**, 032107 (2020).
- [37] S. V. Beentjes and A. Khamseh, *Phys. Rev. E* **102**, 053314 (2020).
- [38] D. Wu, L. Wang, and P. Zhang, *Phys. Rev. Lett.* **122**, 080602 (2019).
- [39] R. Fournier, L. Wang, O. V. Yazyev, and Q. Wu, *Phys. Rev. Lett.* **124**, 056401 (2020).
- [40] G. J. Percebois and D. Weinmann, *Phys. Rev. B* **104**, 075422 (2021).
- [41] X.-Y. Dong, F. Pollmann, and X.-F. Zhang, *Phys. Rev. B* **99**, 121104 (2019).
- [42] R. Zhang, B. Wei, D. Zhang, J.-J. Zhu, and K. Chang, *Phys. Rev. B* **99**, 094427 (2019).
- [43] A. Canabarro, F. F. Fanchini, A. L. Malvezzi, R. Pereira, and R. Chaves, *Phys. Rev. B* **100**, 045129 (2019).
- [44] M. Jo, J. Lee, K. Choi, and B. Kahng, *Phys. Rev. Research* **3**, 013238 (2021).
- [45] W.-C. Guo, B.-Q. Ai, and L. He, *Europhys. Lett.* **136**, 48002 (2021).
- [46] See Supplemental Material, which includes Refs. [16, 70–72], for more information on data generation, NN training, investigation on LFRU's robustness against different choices of the NN architecture, a blank comparison, and the NN's performance on ISP.
- [47] J. B. Kogut, *Rev. Mod. Phys.* **51**, 659 (1979).
- [48] K. Amann-Winkel, R. Böhmer, F. Fujara, C. Gainaru, B. Geil, and T. Loerting, *Rev. Mod. Phys.* **88**, 011002 (2016).
- [49] P. Digregorio, D. Levis, A. Suma, L. F. Cugliandolo, G. Gonnella, and I. Pagonabarraga, *Phys. Rev. Lett.* **121**, 098003 (2018).
- [50] Y.-W. Li and M. P. Ciamarra, *Phys. Rev. Lett.* **124**, 218002 (2020).
- [51] R.-Y. Sun and Z. Zhu, *Phys. Rev. B* **104**, L121118 (2021).
- [52] J. Wang, L. Zhang, R. Ma, Q. Chen, Y. Liang, and T. Ma, *Phys. Rev. B* **101**, 245161 (2020).
- [53] A. J. Fontenele, N. A. P. de Vasconcelos, T. Feliciano, L. A. A. Aguiar, C. Soares-Cunha, B. Coimbra, L. Dalla Porta, S. Ribeiro, A. J. a. Rodrigues, N. Sousa, P. V. Carelli, and M. Copelli, *Phys. Rev. Lett.* **122**, 208101 (2019).
- [54] J. M. Kosterlitz, *Rep. Prog. Phys.* **79**, 026001 (2016).
- [55] J. M. Kosterlitz and D. J. Thouless, *J. Phys. C* **6**, 1181 (1973).
- [56] J. M. Kosterlitz, *J. Phys. C* **7**, 1046 (1974).
- [57] Y. Kumano, K. Hukushima, Y. Tomita, and M. Oshikawa, *Phys. Rev. B* **88**, 104427 (2013).
- [58] S. K. Baek, H. Mäkelä, P. Minnhagen, and B. J. Kim, *Phys. Rev. E* **88**, 012125 (2013).
- [59] S. Hong and D.-H. Kim, *Phys. Rev. E* **101**, 012124 (2020).

- [60] C.-O. Hwang, Phys. Rev. E **80**, 042103 (2009).
- [61] Z.-Q. Li, L.-P. Yang, Z. Y. Xie, H.-H. Tu, H.-J. Liao, and T. Xiang, Phys. Rev. E **101**, 060105 (2020).
- [62] Y. Miyajima, Y. Murata, Y. Tanaka, and M. Mochizuki, Phys. Rev. B **104**, 075114 (2021).
- [63] L. Hostetler, J. Zhang, R. Sakai, J. Unmuth-Yockey, A. Bazavov, and Y. Meurice, Phys. Rev. D **104**, 054505 (2021).
- [64] K. He, X. Zhang, S. Ren, and J. Sun, in *Proceedings of the 2016 IEEE Conference on Computer Vision and Pattern Recognition* (IEEE CVPR, Las Vegas, 2016) pp. 770–778.
- [65] C. Szegedy, W. Liu, Y. Jia, P. Sermanet, S. Reed, D. Anguelov, D. Erhan, V. Vanhoucke, and A. Rabinovich, in *Proceedings of the 2015 IEEE Conference on Computer Vision and Pattern Recognition* (IEEE CVPR, Boston, 2015) pp. 1–9.
- [66] H. Chaté, Annu. Rev. Condens. Matter Phys. **11**, 189 (2020).
- [67] M. A. Muñoz, Rev. Mod. Phys. **90**, 031001 (2018).
- [68] C. Bechinger, R. Di Leonardo, H. Löwen, C. Reichhardt, G. Volpe, and G. Volpe, Rev. Mod. Phys. **88**, 045006 (2016).
- [69] T. Vicsek and A. Zafeiris, Phys. Rep. **517**, 71 (2012).
- [70] R. H. Swendsen and J.-S. Wang, Phys. Rev. Lett. **58**, 86 (1987).
- [71] J.-S. Wang and R. H. Swendsen, Phys. A: Stat. Mech. Appl. **167**, 565 (1990).
- [72] D. P. Kingma and J. Ba, in *Proceedings of the 3rd International Conference on Learning Representations* (ICLR, San Diego, 2015).

Supplemental Material for “Learning Phase Transitions from Regression Uncertainty”

Wei-chen Guo and Liang He*

Guangdong Provincial Key Laboratory of Quantum Engineering and Quantum Materials,
 School of Physics and Telecommunication Engineering,
 South China Normal University, Guangzhou 510006, China and
 Guangdong-Hong Kong Joint Laboratory of Quantum Matter,
 South China Normal University, Guangzhou 510006, China

DATA GENERATION AND NEURAL NETWORK TRAINING

In this work, the data generation for the ferromagnetic Ising model is done by Monte Carlo simulations using the Swendsen-Wang algorithm [1, 2] on the Ising Hamiltonian H with periodic boundary condition imposed. For the ferromagnetic Ising model with each system size $L = 120, 140, 160, 180$, we generate 7×10^3 samples of the steady state configuration at each temperature T in the temperature region $[2.0, 2.5]$ with the temperature spacing kept as $\Delta T = 0.02$, respectively. These samples are converted to images as shown in Fig. 1(a) in the main text, where the blue or red at each pixel represents the spin s_i on the i th lattice site, and then divided into three categories in the ratio of 5:1:1 forming the training, validation, and test datasets [3].

The data generation for the q -state clock model is done by Monte Carlo simulations on the Hamiltonian H_q with periodic boundary condition imposed. For $q = 6, 7$ and $L = 100$, we generate 7×10^3 samples of the steady state configuration at each temperature T in the temperature region $[0.2, 1.4]$ with $\Delta T = 0.02$, respectively. These samples are also converted to images as shown in Fig. 2(a) in the main text, where the cyclic color at each pixel represents the planar angle θ_i on the i th lattice site, and then divided into three categories in the same ratio as above forming the datasets.

Using these datasets, we employ two widely-used standard neural networks (NNs) called “ResNet” (whose results are shown in Fig. 1 and Fig. 2 in the main text) and “GoogLeNet” (whose results are shown in Figs. S1, S2) to perform regression tasks of inverse statistical problem (ISP). They are trained by using the Adam optimizer [4] traversing the training dataset for 10 epochs at learning rate $\alpha = 10^{-3}$, together with a validation at each epoch traversing the validation dataset. After that, the samples in the test datasets are used to calculate the regression uncertainty $U(T)$. All the machine learning results in this work are averaged over 20 independent training and testing processes.

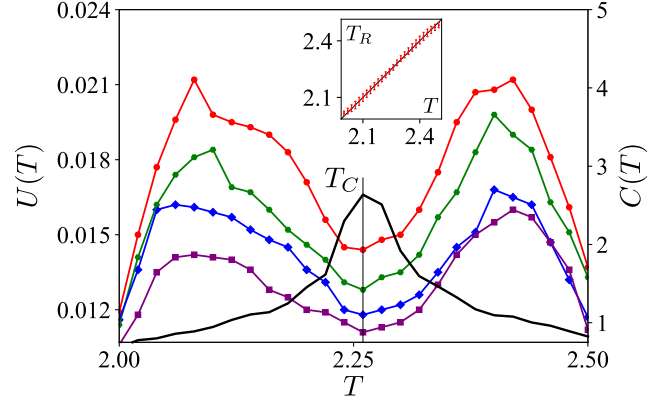


Figure S1. Analogous data to Fig. 1(b), but employing another type of widely-used standard NN called “GoogLeNet” instead of “ResNet”. See text for more details.

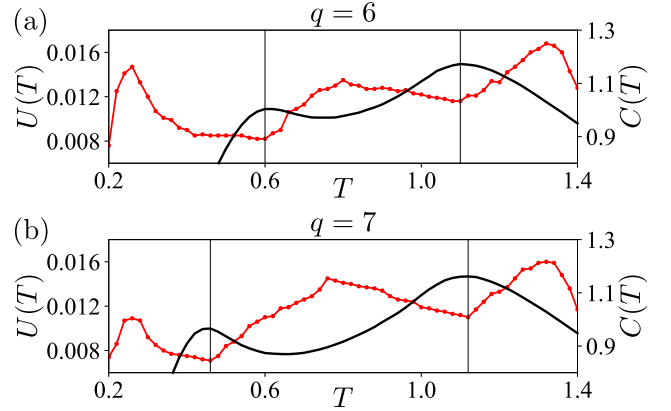


Figure S2. Analogous data to Figs. 2(b), (c), but employing “GoogLeNet” instead of “ResNet”. These two employed NNs have very different designs for the feature extraction, but their results match very well, manifesting that the implementation of LFRU is robust against different choices of the NN architecture. See text for more details.

BLANK COMPARISON

For a blank comparison, we apply our new approach “learning from regression uncertainty” (LFRU) on the ferromagnetic Ising model concerning solely the low temperature region $[2.0, 2.2]$ employing both “ResNet” and “GoogLeNet”, respectively, and find in Fig. S3(a) that the temperature dependence of regression uncertainty $U(T)$ assumes a single maximum and no non-trivial minimum.

* liang.he@sncu.edu.cn

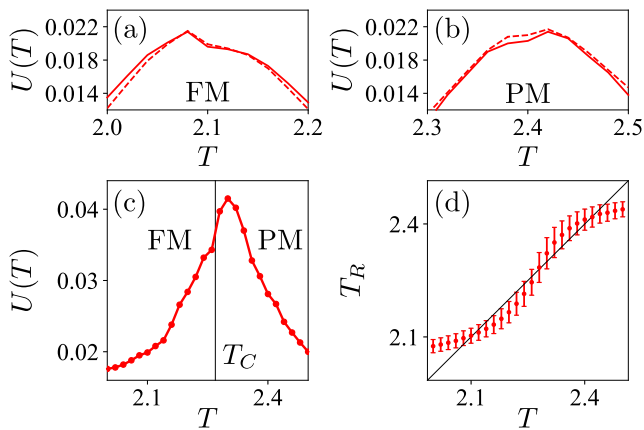


Figure S3. (a) Temperature dependence of regression uncertainty $U(T)$ for the ferromagnetic Ising model with $L = 120$, but concerning solely the low temperature region $[2.0, 2.2]$. Only the ferromagnetic (FM) phase exists in this region, so the curve of $U(T)$ assumes no non-trivial minimum. Solid line: “ResNet”. Dashed line: “GoogLeNet”. (b) Analogous data to (a), but corresponding to the high temperature region $[2.3, 2.5]$, where only the paramagnetic (PM) phase exists. (c) Temperature dependence of regression uncertainty $U(T)$ concerning $[2.0, 2.5]$ on the ferromagnetic Ising model with system size $L = 120$ obtained by using a very simple fully connected NN for a deliberately produced poor performance on ISP. This curve of $U(T)$ looks similar as (a) and (b), suggesting that one cannot distinguish whether a single peak of $U(T)$ is associated with a phase transition or not merely by monitoring the regression uncertainty $U(T)$ itself. Therefore, the NN’s good performance on ISP is a prerequisite of LFRU for identifying phase transitions. (d) The NN’s poor performance on ISP corresponding to (c). The reconstructed temperature T_R (red) largely departs from the target T (black diagonal line). See text for more details.

This is consistent with the fact that only one phase, i.e., the ferromagnetic phase, exists with no phase transition in the temperature region $[2.0, 2.2]$. The similar results are obtained concerning solely the high temperature region $[2.3, 2.5]$ that corresponds to only the paramagnetic

phase, as shown in Fig. S3(b). These results verify that the non-trivial M-shape structure of the curve of regression uncertainty $U(T)$ shown in Fig. 1(b) in the main text is indeed a signal of phase transitions of the system consideration.

PERFORMANCE ON ISP

In LFRU, a connection between regression uncertainty and response properties is revealed, which is the key to the interpretability of LFRU. Here, we note that the revealing of this intrinsic connection is based on the NN’s good performance on ISP. Such a performance is not guaranteed by an arbitrary NN. We deliberately produce a poor performance [cf. Fig. S3(d)] concerning the temperature region $[2.0, 2.5]$ on the ferromagnetic Ising model with system size $L = 120$. This is obtained by using a very simple fully connected NN, which consists of an input layer with $3L^2$ neurons (3 for RGB), a hidden layer with L neurons (rectified linear unit as the activation function, batch normalization applied) [3], and an output layer with only one neuron. It is worth mentioning that the fully connected NN might also perform well after fine-tuning, but a poor performance is needed here for technical discussions.

As we can see from Fig. S3(c), when the NN cannot well accomplish its task of ISP, the resulting temperature dependence of regression uncertainty $U(T)$ looks similar as the results in Figs. S3(a) and S3(b) concerning solely the temperature region where no phase transition exists. However, the temperature region $[2.0, 2.5]$ under consideration is across the critical temperature $T_C \approx 2.269$, suggesting that one cannot distinguish whether a single peak of $U(T)$ is associated with a phase transition or not merely by monitoring the regression uncertainty $U(T)$ itself. A reasonable judgment is that any investigation according to the information extracted from a poor performance would suffer from the lack of legitimacy. In this regard, the NN’s good performance on ISP is a prerequisite of LFRU for identifying phase transitions.

[1] R. H. Swendsen and J.-S. Wang, Phys. Rev. Lett. **58**, 86 (1987).

[2] J.-S. Wang and R. H. Swendsen, Phys. A: Stat. Mech. Appl. **167**, 565 (1990).

[3] I. Goodfellow, Y. Bengio, and A. Courville, *Deep Learning* (MIT Press, Cambridge, 2016).

[4] D. P. Kingma and J. Ba, in *Proceedings of the 3rd International Conference on Learning Representations (ICLR, San Diego, 2015)*.